

## Paramagnetic Anisotropy and Crystal-Field Splittings in $\text{EuAlO}_3$

L. HOLMES, R. SHERWOOD, AND L. G. VAN UITERT  
*Bell Telephone Laboratories, Murray Hill, New Jersey 07974*

AND

S. HÜFNER\*  
*Institute für Technische Physik, Darmstadt, Germany*  
 (Received 13 August 1968)

The magnetic susceptibilities for orthorhombic  $\text{EuAlO}_3$  have been measured between 1.5 and 300°K. The compound is paramagnetic and shows approximately 20% anisotropy in the susceptibilities below 100°K. The susceptibility along the  $b$  axis has a very broad maximum at  $T \sim 60^\circ\text{K}$ . Optical fluorescence and absorption measurements show the  ${}^7F_1$  levels for  $\text{Eu}^{3+}$  at 281, 359, and 479  $\text{cm}^{-1}$ . The susceptibilities, extrapolated to  $T=0^\circ\text{K}$ , are fitted with theoretical formulas based on the observed splittings of the  ${}^7F_1$  levels.

### INTRODUCTION

THE magnetic behavior of the ion  $\text{Eu}^{3+}$  has been of classic interest in the field of magnetism. The paramagnetic susceptibility was first explained satisfactorily when Van Vleck's formula<sup>1</sup> for  $\chi$  was applied<sup>2</sup> to this ion. More recently, there has been extensive interest in the behavior of  $\text{Eu}^{3+}$  as a magnetic sublattice in europium iron garnet ( $\text{Eu}_3\text{Fe}_5\text{O}_{12}$ ).<sup>3</sup> The present experiments on  $\text{EuAlO}_3$  are, to our knowledge, the first in which anisotropy has been observed in the magnetic susceptibility of  $\text{Eu}^{3+}$ .

The magnetic properties of rare-earth ions in "distorted perovskite" structures are profoundly influenced by crystal fields.<sup>4</sup> In these compounds, 15 parameters are needed to describe the splittings of the rare-earth levels. For the ion  $\text{Eu}^{3+}$ , only two of these parameters affect the magnetic susceptibilities at low temperatures, to first order in the crystal field. The parameters involved are the coefficients of the second-degree rhombic field, which splits the  ${}^7F_1$  manifold for  $\text{Eu}^{3+}$ . To study these effects, single crystals of  $\text{EuAlO}_3$  have been prepared and the positions of the low-lying energy levels determined from optical absorption and fluorescence. The (anisotropic) magnetic susceptibilities have been measured between 1.5 and 300°K and the results compared with theoretical formulas based on the crystal-field splittings.

### RESULTS

Single crystals of  $\text{EuAlO}_3$  were prepared from high-purity oxides using a  $\text{PbO-PbF}_2\text{-B}_2\text{O}_3$  flux. Flux-free and colorless crystals were selected from two batches for the measurements.

\* Work partially done at Bell Telephone Laboratories, Murray Hill, N. J.

<sup>1</sup> J. H. Van Vleck, *Theory of Electric and Magnetic Susceptibilities* (Oxford University Press, London, 1932), p. 248.

<sup>2</sup> J. H. Van Vleck and A. Frank, *Phys. Rev.* **34**, 1494 (1929); **34**, 1625 (1929).

<sup>3</sup> For a review of this work, see J. H. Van Vleck, *J. Appl. Phys.* **39**, 1 (1968).

<sup>4</sup> The magnetic properties of a number of these compounds are described in a series of papers by various authors, *J. Appl. Phys.* **39**, 1360-1374 (1968).

The spectroscopic measurements were performed with a 2m-grating spectrograph. The samples were immersed directly in liquid nitrogen ( $T=77^\circ\text{K}$ ). The positions of the  ${}^7F_1$  excited states (Fig. 1) were determined from absorption measurements of the  ${}^7F_1 \rightarrow {}^5D_0$  transitions, and checked against those obtained from the  ${}^5D_0 \rightarrow {}^7F_1$  fluorescence transitions. The results of these two measurements agreed within the experimental accuracy of  $\pm 0.4 \text{ cm}^{-1}$ . The measurements showed the  ${}^7F_1$  level for the free-ion split into three singlets at 281, 359, and 479  $\text{cm}^{-1}$ , respectively. The positions of four of the  ${}^7F_2$  levels (Fig. 1) was determined from fluorescence measurements of the  ${}^5D_0 \rightarrow {}^7F_2$  transitions. The transition to the fifth level was either too weak to be seen or degenerate with one of the other four. The center of gravity of the  ${}^7F_2$  levels is at approximately 1000  $\text{cm}^{-1}$ .<sup>5</sup>

Magnetization data in the principal crystallographic directions were obtained with a pendulum magnetometer. The curves (Fig. 2) show roughly 20% anisotropy below 100°K. The small  $C/T$  "tail" at low temperatures could be caused by trace amounts of almost any magnetic impurity. The magnitude of the tail corresponds to less than 0.005 at.% of divalent europium. By extrapolating from above 10°K, values are obtained

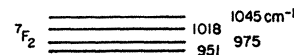
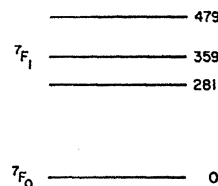


FIG. 1. Low-lying energy levels for  $\text{Eu}^{3+}$  in  $\text{EuAlO}_3$ .



<sup>5</sup> This value may be compared with 1050  $\text{cm}^{-1}$  in europium ethylsulfate [E. V. Sayre and S. Freed, *J. Chem. Phys.* **24**, 1213 (1956)] and 975  $\text{cm}^{-1}$  in yttrium gallium garnet [J. A. Koningstein, *J. Chem. Phys.* **42**, 3195 (1965)].

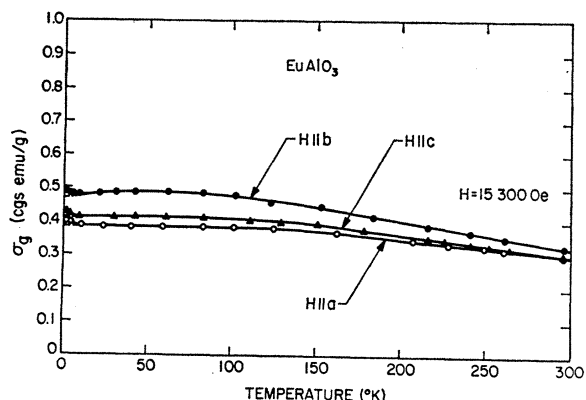


FIG. 2. Magnetization along  $a$ ,  $b$ , and  $c$  axes in paramagnetic  $\text{EuAlO}_3$ .

for the magnetic susceptibilities  $\chi = \sigma/H$  at  $T=0^\circ\text{K}$ . The values are  $5.68$ ,  $6.97$ , and  $6.11 \times 10^{-3}$  cgs emu/mole, respectively, in the  $a$ ,  $b$ , and  $c$  directions.

### INTERPRETATION

The crystal structure for  $\text{EuAlO}_3$  is orthorhombic  $D_{2h}^{16}(\text{Pbnm})$ .<sup>6</sup> The rare-earth ions are on two magnetically inequivalent sites of monoclinic point symmetry  $C_{1h}$ . The principal magnetic axes for these sites are related by a mirror reflection in the  $a$ - $c$  plane. We define the local magnetic axes as shown in Fig. 3, with the local  $z$  axis along the crystallographic  $c$  axis. The susceptibility along the  $c$  axis of the crystal measures the susceptibility  $\chi_z$  along the local  $z$  axis, whereas the susceptibilities along  $a$  and  $b$  give linear combinations of  $\chi_x$  and  $\chi_y$  for the two sites.

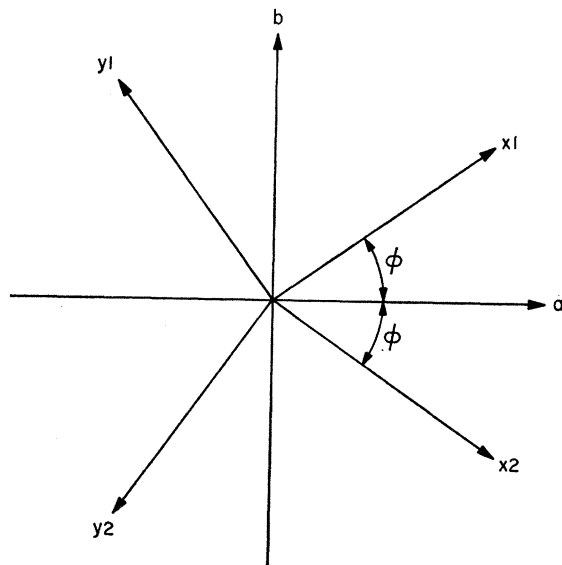


FIG. 3. Principal magnetic axes for the two inequivalent sites for  $\text{Eu}^{3+}$  in  $\text{EuAlO}_3$ . The  $z$  axis is coincident with the crystallographic  $c$  axis, while the  $x$  and  $y$  axes for the two sites are related by a mirror reflection in the  $a$ - $c$  plane.

<sup>6</sup> S. Geller and V. B. Bala, *Acta Cryst.* **9**, 1019 (1956).

The ground state for  $\text{Eu}^{3+}$  is the singlet  ${}^7F_0$ , and the first excited state is the triply degenerate  ${}^7F_1$ . At low temperatures, all of the susceptibility arises from second-order mixing of the  ${}^7F_1$  levels into the ground state. For free ions

$$\chi(T=0^\circ\text{K}) = 8N\beta^2/\Delta_{10}, \quad (1)$$

where  $\Delta_{10}$  is the interval in energy between the  $J=0$  and  $J=1$  levels.<sup>1</sup>

In  $\text{EuAlO}_3$ ,  $\chi(T=0^\circ\text{K})$  is influenced by crystal fields and by exchange interactions. The fractional increment in  $\chi$  produced by isotropic exchange at low temperatures may be written<sup>7,8</sup>

$$\Delta\chi_{\text{ex}}/\chi(T=0^\circ\text{K}) = 16 \sum_j J_{ij}/\Delta_{10},$$

where  $J_{ij}$  is the exchange parameter for neighboring  $\text{Eu}^{3+}$  ions. Using  $J_{ij}/k \sim -0.07^\circ\text{K}$ , as determined<sup>9</sup> in  $\text{GdAlO}_3$ , we find

$$\Delta\chi_{\text{ex}}/\chi(T=0^\circ\text{K}) \sim -1\%,$$

which is within the experimental uncertainty. Anisotropic exchange, which can give a net isotropic coupling in a cubic crystal, has been examined by Van Vleck and Huang<sup>7</sup> for  $\text{Eu}_2\text{O}_3$ . There, the anisotropic contributions may be significant, but the isotropic exchange is also several times larger than in  $\text{EuAlO}_3$ . We shall neglect any exchange contributions to  $\chi(T=0^\circ\text{K})$ .

In a crystal field, the degeneracy of the  ${}^7F_1$  levels is lifted (Fig. 1). For a powder sample or for a cubic crystal, Eq. (1) is still valid to first order in the crystal field, providing only that  $\Delta_{10}$  is replaced by  $\bar{\Delta}_{10}$ , the center of gravity of the  ${}^7F_1$  levels.<sup>10</sup> In  $\text{EuAlO}_3$ , which is orthorhombic, the susceptibility is anisotropic. A magnetic field along one of the local principal axes (Fig. 3) couples only one of the  ${}^7F_1$  singlets into the ground state. The anisotropy is of the order of magnitude of the splitting of the  ${}^7F_1$  levels ( $\sim 100 \text{ cm}^{-1}$ ), divided by  $\bar{\Delta}_{10}$  ( $\sim 400 \text{ cm}^{-1}$ ), or 25%.

An approximation to  $\chi_\epsilon(T=0^\circ\text{K})$ , where  $\epsilon = x, y, \text{ or } z$ , is obtained by including all contributions which are of first order in the crystal field. In principle, fifteen<sup>11</sup> crystal-field parameters  $V_n^m$  are required to describe the splitting of the  $\text{Eu}^{3+}$  levels in the monoclinic crystal field. Only the second-degree rhombic parameters  $V_2^0$  and  $V_2^2$  contribute in first order to  $\chi_\epsilon(T=0^\circ\text{K})$ . The second-degree rhombic portion  $V^{(2)}$  of the crystal

<sup>7</sup> J. H. Van Vleck and N. L. Huang, to be published by the French Physical Society in the Jubilee book in honor of Professor A. Kastler.

<sup>8</sup> W. P. Wolf and J. H. Van Vleck, *Phys. Rev.* **118**, 1490 (1960).

<sup>9</sup> J. D. Cashion, A. H. Cooke, J. F. B. Hawkes, M. J. M. Leask, T. L. Thorp, and M. R. Wells, *J. Appl. Phys.* **39**, 1360 (1968).

<sup>10</sup> M. Schieber and L. Holmes, *J. Appl. Phys.* **36**, 1159 (1965); A. Frank, *Phys. Rev.* **48**, 765 (1935).

<sup>11</sup> It is always possible to choose the coordinate system in such a way that one of the parameters is eliminated. We have, for convenience, eliminated  $V_2^{-2}$  in that way. For a discussion of this point, see J. B. Gruber, W. F. Krupke, and J. M. Poindexter, *J. Chem. Phys.* **41**, 3363 (1964).

potential may be written

$$V^{(2)} = \alpha_J V_2^0 O_2^0 + \alpha_J V_2^2 O_2^2, \quad (2)$$

where  $O_n^m$  are operator equivalents,  $V_n^m \equiv A_n^m \langle r^n \rangle$  are the crystal-field parameters, and  $\alpha_J$  is the Stevens constant.<sup>12</sup> The  ${}^7F_1$  levels are split by  $V^{(2)}$  into three singlets. The energy levels for these three singlets may be written  $\Delta_\epsilon$ , where  $\epsilon = x, y,$  and  $z$ :

$$\begin{aligned} \Delta_x - \bar{\Delta}_{10} &= -\frac{1}{5}(V_2^0 - V_2^2), \\ \Delta_y - \bar{\Delta}_{10} &= -\frac{1}{5}(V_2^0 + V_2^2), \\ \Delta_z - \bar{\Delta}_{10} &= \frac{2}{5}V_2^0, \end{aligned} \quad (3)$$

to first order in  $V^{(2)}$ . In this approximation, a magnetic field along the local  $\epsilon$  axis (Fig. 3) connects the ground state only with the  ${}^7F_1$  singlet at energy  $\Delta_\epsilon$ . An expression for  $\chi_\epsilon(T=0^\circ\text{K})$  is derived in the Appendix. In terms of the first-order splittings (3) of the  ${}^7F_1$  levels,

$$\chi_\epsilon(T=0^\circ\text{K}) = \frac{8N\beta^2}{\Delta_\epsilon} \left(1 - \frac{\Delta_\epsilon - \bar{\Delta}_{10}}{\bar{\Delta}_{20}}\right)^2, \quad (4)$$

where  $\bar{\Delta}_{20}$  is the center of gravity of the  ${}^7F_2$  levels. The factor in parentheses arises from mixing of the  ${}^7F_2$  levels into the ground state by the crystal field.

The expression for  $\chi_\epsilon$  in (4) is accurate to first order in  $V^{(2)}$ . Additional second-order contributions arising from the mixing of levels with  $J \geq 2$  into the  $J=0$  and  $J=1$  levels have been neglected. An estimate of the change  $\Delta\chi$  produced by these terms is given by

$$\Delta\chi/\chi \sim \frac{1}{3} \sum_{\epsilon=x,y,z} \left(\frac{\Delta_\epsilon - \Delta_{10}}{\bar{\Delta}_{10}}\right)^2 \sim 5\%.$$

Taking  $\bar{\Delta}_{20} = 1000 \text{ cm}^{-1}$ , we calculate from (4) a spatial-average or "powder" susceptibility of  $6.10 \times 10^{-3}$  cgs emu/mole, which is 2.5% smaller than the measured value of  $6.25 \times 10^{-3}$  in  $\text{EuAlO}_3$ .

The susceptibilities along  $a, b,$  and  $c$  are related to the susceptibilities along the local axes in  $\text{EuAlO}_3$  as follows:

$$\begin{aligned} \chi_a &= \chi_x \cos^2\phi + \chi_y \sin^2\phi, \\ \chi_b &= \chi_x \sin^2\phi + \chi_y \cos^2\phi, \\ \chi_c &= \chi_z. \end{aligned} \quad (5)$$

The angle  $\phi$  is the angle between the  $a$  axis of the crystal and the local  $x$  axis (see Fig. 3). To fit the observed anisotropies, we must choose  $\Delta_x = 359 \text{ cm}^{-1}$  (Fig. 1). Choosing  $\Delta_x = 479 \text{ cm}^{-1}$  and  $\Delta_y = 281 \text{ cm}^{-1}$  gives  $\phi < 45^\circ$ . Figure 4 shows a plot of Eqs. (5) for this choice of  $\Delta_x$  and  $\Delta_y$ , and with  $\bar{\Delta}_{20} = 1000 \text{ cm}^{-1}$ . Subtracting  $\chi_p = \frac{1}{3}(\chi_x + \chi_y + \chi_z)$  from the experimental and theoretical points (as done in Fig. 4) tends to minimize the second-order contributions which have been neglected. The best fit is obtained for  $\phi = 38^\circ$ . The calculated sus-

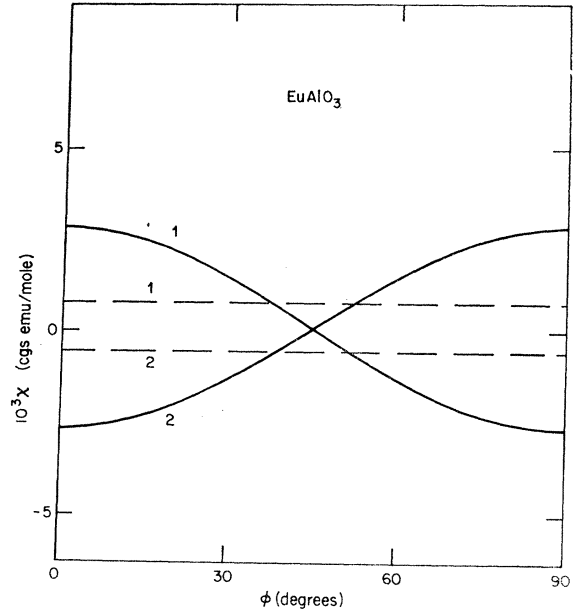


FIG. 4. Magnetic susceptibilities at  $0^\circ\text{K}$  along the  $a$  and  $b$  axes in  $\text{EuAlO}_3$ . Solid curves (theory): 1:  $(\chi_b - \chi_p)$ ; 2:  $(\chi_a - \chi_p)$ . Dashed lines (experiment): 1:  $(\chi_b - \chi_p)$ ; 2:  $(\chi_a - \chi_p)$ . Powder susceptibility,  $\chi_p = \frac{1}{3}(\chi_x + \chi_y + \chi_z)$ .

ceptibilities, summarized in Table I, show good agreement with the data.

#### MAXIMUM IN $\chi$

The magnetization for  $H \parallel b$  (Fig. 2) rises to a very broad maximum at  $T \sim 60^\circ\text{K}$ . The susceptibility at the maximum is  $7.21 \times 10^{-3}$  cgs emu/mole, which is 3% higher than the extrapolated value at  $T=0^\circ\text{K}$ , and 1% higher than the value measured at  $20^\circ\text{K}$ . Since the effect is small, it is perhaps unwise to attach a great deal of significance to it. It is interesting to note, however, that a maximum in  $\chi$  for  $\text{Eu}^{3+}$  was predicted from a theoretical study<sup>13</sup> of dynamic spin-phonon coupling in the garnet structure. The effect was not observed in garnet. In  $\text{EuAlO}_3$ , the (anisotropic) susceptibility is more sensitive to the static crystal field than is the (isotropic) susceptibility in Eu garnet. It could be that dynamic spin-phonon coupling would also show up more clearly in  $\text{EuAlO}_3$ .

There may be other explanations for the maximum. The Van Vleck theory predicts a maximum (much smaller than we observe) at about  $80^\circ\text{K}$  for free ions,

TABLE I. Magnetic susceptibilities per mole extrapolated to  $0^\circ\text{K}$  in  $\text{EuAlO}_3$ .

	$a$ axis		$b$ axis		$c$ axis	
	Expt	Theory	Expt	Theory	Expt	Theory
$10^3(\chi - \chi_p)^a$	-0.57	-0.61	0.72	0.73	-0.14	-0.12
$10^3\chi$	5.68	5.49	6.97	6.83	6.11	5.98

<sup>a</sup>  $\chi_p = \frac{1}{3}(\chi_x + \chi_y + \chi_z)$ .

<sup>12</sup> M. T. Hutchings, in *Solid State Physics*, edited by F. Seitz and D. Turnbull (Academic Press Inc., New York, 1964), Vol. 16, p. 227.

<sup>13</sup> R. Orbach and P. Pincus, *Phys. Rev.* **143**, 168 (1966).

due to the influence of the  ${}^7F_1$  levels.<sup>14</sup> The predicted increase in  $\chi$  over  $\chi(T=0^\circ\text{K})$  is about 0.09%. This effect would be enhanced by antiferromagnetic exchange interactions. An exchange field is more effective, relative to an applied field, for  $\text{Eu}^{3+}$  ions in the ground state than for  $\text{Eu}^{3+}$  ions in the  ${}^7F_1$  states.<sup>8</sup> To see how this goes, we have assumed an exchange field  $H_{\text{ex}}$  proportional to the average spin,<sup>14</sup> and calculated the magnetization in external plus exchange fields, using the formula of Wolf and Van Vleck.<sup>8</sup> The magnitude of  $H_{\text{ex}}$  was chosen to give a one percent decrease in  $\chi(T=0^\circ\text{K})$ , which is the order of magnitude expected in  $\text{EuAlO}_3$ . In this case, the magnetization increases by about 0.095% between  $T=0$  and  $T=80^\circ\text{K}$ .

It should be mentioned that anisotropy in the exchange, as discussed by Van Vleck and Huang,<sup>7</sup> would influence the  ${}^7F_1$  and  ${}^7F_0$  levels differently. This would also affect the dependence of  $\chi$  on temperature. To fully explore these questions in  $\text{EuAlO}_3$  would require a knowledge of all contributions to  $\chi$  at low temperatures from the static crystal field.

### DISCUSSION

The magnetic susceptibility of  $\text{EuAlO}_3$  is anisotropic because of the low (orthorhombic) crystal symmetry. The anisotropy is big enough to measure because of the anomalously large splitting of the  ${}^7F_1$  levels in the monoclinic crystal field. The size of the parameters  $V_2^0$  and  $V_2^2$ , which split the  ${}^7F_1$  levels, may be estimated from Eqs. (3). We find  $V_2^0 \sim -35 \text{ cm}^{-1}$  and  $V_2^2 \sim \pm 500 \text{ cm}^{-1}$ , with the axis of quantization along the  $c$  axis of the crystal (i.e.,  $\Delta_z = 359 \text{ cm}^{-1}$ ). Transforming the axis of quantization into the  $a$ - $b$  plane (to give  $\Delta_{z'} = 479 \text{ cm}^{-1}$ ) we find  $V_2^{0'} \sim 265 \text{ cm}^{-1}$  and  $V_2^{2'} \sim \pm 200 \text{ cm}^{-1}$ . These values may be compared with  $V_2^0 = (195 \pm 40)$  and  $(159 \pm 40) \text{ cm}^{-1}$ , respectively, deduced from Mössbauer absorption spectra in the isomorphous compounds  $\text{DyFeO}_3$ <sup>15</sup> and  $\text{DyCrO}_3$ .<sup>16</sup>

In  $\text{EuAlO}_3$ , the local axes make an angle of approximately  $38^\circ$  with the  $a$  and  $b$  axes of the crystal. This may be compared to the angle  $35^\circ$  determined<sup>17</sup> in  $\text{TbAlO}_3$  and the angle  $33^\circ$  determined<sup>18</sup> in  $\text{DyAlO}_3$ . Other sources of comparison are the orthoferrites  $\text{DyFeO}_3$  and  $\text{TbFeO}_3$ . In these compounds, the rare-earth moments order antiferromagnetically in the  $a$ - $b$  plane at low temperatures. The  $\text{Dy}^{3+}$  moments lie  $30^\circ$  from the  $b$  axis,<sup>19</sup> whereas the  $\text{Tb}^{3+}$  moments lie  $40^\circ$  from the  $a$  axis.<sup>20</sup> Because of the highly anisotropic nature of the  $\text{Dy}^{3+}$  and  $\text{Tb}^{3+}$  ground states, these angles may be taken

<sup>14</sup> E. D. Jones, *J. Appl. Phys.* **39**, 1090 (1968).

<sup>15</sup> I. Nowik and H. J. Williams, *Phys. Letters* **20**, 154 (1966).

<sup>16</sup> M. Eibschütz and L. G. Van Uitert, *Phys. Rev.* **177**, 502 (1969).

<sup>17</sup> S. Hufner, L. Holmes, F. Varsanyi, and L. G. Van Uitert, *Phys. Rev.* **171**, 507 (1968); and references therein.

<sup>18</sup> H. Schuchert, S. Hufner, and R. Faulhaber, *J. Appl. Phys.* **39**, 1137 (1968).

<sup>19</sup> G. Gorodetsky, B. Sharon, and S. Shtrikman, *J. Appl. Phys.* **39**, 1371 (1968).

<sup>20</sup> J. Mareschal, J. Sivadière, G. F. DeVries, and E. F. Bertaut, *J. Appl. Phys.* **39**, 1364 (1968).

as indicative of the angles between the local axes and the  $a$  and  $b$  axes of the crystal. Considerable variation in angle is observed from compound to compound, as might be expected if the orientation of the local axes is determined largely by the second-degree parameters  $V_2^0$  and  $V_2^2$ . These parameters depend sensitively on the details of the local environment.

The study of  $\text{EuAlO}_3$  has provided new information on the crystal fields in the "distorted perovskites" and on the nature of the magnetic response for  $\text{Eu}^{3+}$ .

### ACKNOWLEDGMENTS

The authors are grateful to Professor J. H. Van Vleck for a preprint of his paper with N. L. Huang and for helpful discussions. We thank R. L. Barns for performing the x-ray orientation and W. Grodkiewicz for assistance in preparing the crystals.

### APPENDIX

In this Appendix, Eq. (4) is derived for a magnetic field along the local  $z$  axis. The result, which is valid to first order in the crystal potential, may be obtained by including (1) the first-order splitting of the  ${}^7F_1$  levels in  $V^{(2)}$ , and (2) the mixing of the  ${}^7F_2$  and  ${}^7F_0$  levels by  $V^{(2)}$ .

The rhombic field described by Eq. (2) splits the  ${}^7F_1$  levels into three singlets which transform under proper rotations as  $x$ ,  $y$ , and  $z$ , respectively:

$$\begin{aligned} |x\rangle &= (|1, 1\rangle - |1, -1\rangle)/\sqrt{2}, \\ |y\rangle &= (|1, 1\rangle + |1, -1\rangle)/\sqrt{2}, \\ |z\rangle &= |1, 0\rangle. \end{aligned}$$

The notation  $|J, M\rangle$  is used for the wave functions of the free ion. The corresponding energy levels are given in Eqs. (3).

To calculate the mixing of the  $J=0$  and  $J=2$  levels, we have used the technique described by Judd.<sup>21</sup> It was first necessary to convert  $V^{(2)}$  to a more general form,<sup>12</sup> since the operator equivalents in Eq. (2) are only valid within a given  $J$ -manifold. For the ground state we find

$$|\psi_0\rangle = |0, 0\rangle - b_{20}|2, 0\rangle - b_{22}(|2, 2\rangle + |2, -2\rangle)/\sqrt{2},$$

to first order in  $V^{(2)}$ , where

$$\begin{aligned} b_{20} &= 4V_2^0/5(3)^{1/2}\bar{\Delta}_{20}, \\ b_{22} &= 4V_2^2/15\bar{\Delta}_{20}. \end{aligned}$$

The magnetic susceptibility may be written<sup>1</sup>

$$\chi_z(T=0^\circ\text{K}) = 2N\beta^2 |\langle \psi_0 | (L_z + 2S_z) | z \rangle|^2 / \Delta_z,$$

where  $\langle \psi_0 | (L_z + 2S_z) | z \rangle = 2 - (3)^{1/2}b_{20}$ . On substituting from Eqs. (3), this reduces to Eq. (4), for  $\epsilon = z$ . The expressions for  $\chi_x$  and  $\chi_y$  are also given correctly by Eq. (4), as follows from a permutation of coordinates.

<sup>21</sup> B. R. Judd, *Operator Techniques in Atomic Spectroscopy* (McGraw-Hill Book Co., New York, 1963).